

# Aza-Crown-Ether-Appended Xanthene: Selective Ratiometric Fluorescent Probe for Silver(I) Ion Based on Arene–Metal Ion Interaction

Ippei Takashima,<sup>†</sup> Anna Kanegae,<sup>†</sup> Manabu Sugimoto,<sup>‡</sup> and Akio Ojida<sup>\*,†</sup>

<sup>†</sup>Graduate School of Pharmaceutical Sciences, Kyushu University, 3-1-1 Maidashi, Higashi-ku, Fukuoka 812-8582, Japan

<sup>‡</sup>Department of Applied Chemistry and Biochemistry, Graduate School of Science and Technology, Kumamoto University, 2-39-1 Kurokami, Chuo-ku, Kumamoto 860-8555, Japan

## Supporting Information

**ABSTRACT:** In this Communication, we report on the development of a ratiometric fluorescent probe for silver(I) ions ( $\text{Ag}^{\text{I}}$ ) based on an arene–metal ion interaction. The probe selectively senses  $\text{Ag}^{\text{I}}$  among various metal ions with a large-emission red shift under aqueous conditions, enabling the selective ratiometric detection of  $\text{Ag}^{\text{I}}$ . X-ray crystallography and NMR analyses reveal that  $\text{Ag}^{\text{I}}$  comes into close contact with the fluorophore, which induces a large-emission red shift. The high sensing selectivity of the probe toward  $\text{Ag}^{\text{I}}$  might be attributable to the restricted rigid conformation of the cyclic aza crown ether, which exclusively binds  $\text{Ag}^{\text{I}}$ . In addition to  $\text{Ag}^{\text{I}}$  sensing, the  $\text{Ag}^{\text{I}}$  complex of the probe is also used for the ratiometric sensing of a cyanide anion ( $\text{CN}^-$ ), highlighting the utility of the reported probe in fluorescence sensing.

Fluorescence probes are essential research tools for analysis of the biological roles and environmental effects of metal ions.<sup>1</sup> The design of these probes is typically based on the functional conjugation of a molecular recognition unit (i.e., ligand unit) and a sensing unit within the same molecule. In such a modular “ligand–(spacer)–fluorophore” design, the sensing selectivity is mainly determined by the binding property of the ligand, and it should be little influenced by the sensing mechanism. However, despite elaborate molecular designs, high sensing selectivity toward specific metal ions is often difficult to achieve solely by modification of the existing ligand structures. Therefore, strong demand exists for a new design strategy of a fluorescent probe to realize the highly selective sensing of specific metal ions.

Recently, we reported a dual-emission fluorescent probe for the detection of metal ions based on a unique fluorescence sensing mechanism.<sup>2</sup> The mechanism consists of an arene–metal ion contact, and it involves a noncoordinating van der Waals contact between the aromatic ring of a fluorophore and a metal ion, which induces a large-emission red shift. We previously reported the design of a type I fluorescent probe (Figure 1), which has two metal-ion binding units such as 2,2′-dipicolylamine on a tricyclic fluorophore. However, the sensing selectivity of these probes was moderate. They sense different metal ions such as  $\text{Cd}^{\text{II}}$ ,  $\text{Ag}^{\text{I}}$ , and  $\text{Hg}^{\text{II}}$ , with a similar large-emission red shift.<sup>2</sup> In this paper, we report a highly selective fluorescent probe for

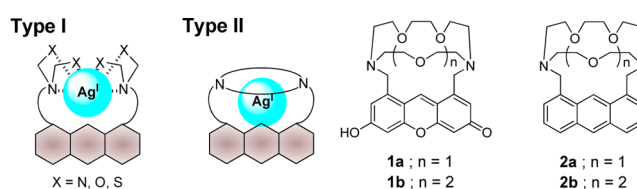


Figure 1. Structures of the compounds.

$\text{Ag}^{\text{I}}$  based on a new molecular design (type II).<sup>3,4</sup> The probe possesses a cyclic aza crown ether as a metal-ion binding unit, and it allows a close arene–metal ion interaction. We found that the xanthene probe with a diaza-15-crown ether **1a** showed a large-emission red shift upon binding to  $\text{Ag}^{\text{I}}$ . A metal-ion screening assay revealed that **1a** showed the high sensing selectivity for  $\text{Ag}^{\text{I}}$  among various metal ions, which has not been achieved by the previously reported fluorescent probes for  $\text{Ag}^{\text{I}}$ .<sup>2,4</sup> X-ray crystallography of the  $\text{Ag}^{\text{I}}$  complex of the anthracene analogue **2a** proved that  $\text{Ag}^{\text{I}}$  was located adjacent to the anthracene ring and thus formed a noncoordinating arene–metal ion contact. In addition to the selective detection of  $\text{Ag}^{\text{I}}$ , the  $\text{Ag}^{\text{I}}$  complex of **1a** was also used for the ratiometric sensing of cyanide anion ( $\text{CN}^-$ ) under aqueous conditions. This highlights the utility of the probe in fluorescence sensing.

The probes possess xanthene (**1a** and **1b**) or anthracene (**2a** and **2b**) as the fluorophore, which is connected to a diaza-15- or -18-crown ether at its 1 and 8 positions. It is expected that this molecular design, which involves a rigidly anchored crown ether with a restricted cyclic conformation and close spatial orientation to the fluorophore, can provide high sensing selectivity toward certain metal ions, based on arene–metal ion contact. The syntheses and fluorescence properties of the probes are described in the Supporting Information (SI; Scheme S1 and Table S1). Figure 2a shows the result of the fluorescence titration of **1a** with  $\text{Ag}^{\text{I}}$  under aqueous buffer conditions [50 mM HEPES (pH 7.4):MeOH = 1:1]. Compound **1a** gave a clear ratiometric signal change upon binding to  $\text{Ag}^{\text{I}}$ , and the emission wavelength red-shifted from 524 nm, 19084  $\text{cm}^{-1}$ , to 554 nm, 18051  $\text{cm}^{-1}$  ( $\Delta\lambda_{\text{em}} = 30$  nm, 1033  $\text{cm}^{-1}$ ). The ratio  $R = F_{554}/F_{524}$  increased from 0.32 to 11.0 upon binding to  $\text{Ag}^{\text{I}}$ . This emission wavelength shift coincided with the absorbance red shift ( $\Delta\lambda_{\text{abs}} = 14$  nm, 521

Received: April 29, 2014

Published: July 9, 2014

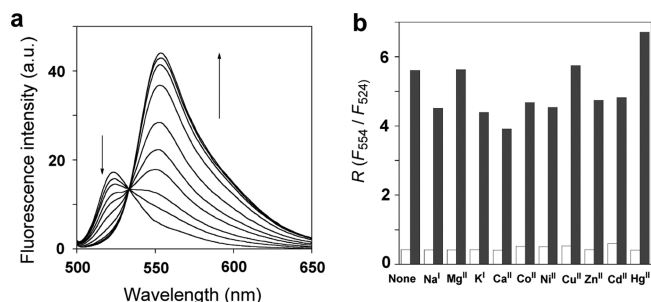


**Figure 2.** (a) Fluorescence spectral change of **1a** ( $5 \mu\text{M}$ ) upon the addition of  $\text{Ag}^+$  (0–10 equiv). Measurement conditions: 50 mM HEPES buffer (pH 7.4):MeOH (1:1),  $\lambda_{\text{ex}} = 488 \text{ nm}$ ,  $25^\circ\text{C}$ . (b) Fluorescence sensing selectivity of **1a** ( $5 \mu\text{M}$ ) for various metal ions. The white bar represents the ratio  $R (F_{554}/F_{524})$  upon the addition of each metal ion (100 equiv). The gray bar represents the ratio  $R (F_{554}/F_{524})$  upon the addition of  $\text{Ag}^+$  (10 equiv) in the presence of other metal ions (100 equiv). Measurement conditions: 50 mM HEPES (pH 7.4),  $\lambda_{\text{ex}} = 488 \text{ nm}$ ,  $25^\circ\text{C}$ .

$\text{cm}^{-1}$ ; Figure S1 in the SI), indicating that the photophysical property of **1a** was modulated by  $\text{Ag}^+$  coordination in the ground state. The fluorescence Job's plot confirmed that the binding stoichiometry between **1a** and  $\text{Ag}^+$  was 1:1 (Figure S2 in the SI). The binding constant ( $K_a, \text{M}^{-1}$ ) of **1a** with  $\text{Ag}^+$  was determined to be  $4.53 \times 10^5 \text{ M}^{-1}$  by a curve-fitting analysis of the titration data. The detection limit for  $\text{Ag}^+$  was 65.6 nM ( $3\sigma$ ). This sensing property was not significantly affected by the presence of various anion species (Table S2 in the SI). Probe **1b**, which possesses a diaza-18-crown ether, also showed an emission red shift upon binding to  $\text{Ag}^+$  with a 1:1 binding stoichiometry ( $K_a = 2.89 \times 10^5 \text{ M}^{-1}$ ; Figures S2 and S3 in the SI). However, the emission wavelength shift ( $\Delta\lambda_{\text{em}} = 10 \text{ nm}$ ,  $354 \text{ cm}^{-1}$  from  $526 \text{ nm}$ ,  $19011 \text{ cm}^{-1}$ , to  $536 \text{ nm}$ ,  $18657 \text{ cm}^{-1}$ ) and the ratio change ( $\Delta R = 0.77$  from 0.74 to 1.51) induced by  $\text{Ag}^+$  were smaller than those of **1a** ( $\Delta\lambda_{\text{em}} = 30 \text{ nm}$ ,  $1033 \text{ cm}^{-1}$ ;  $\Delta R = 10.7$ ). Compound **1a** with a superior ratiometric signal change is thus more suitable for the detection of  $\text{Ag}^+$  than **1b**. The metal-ion-sensing selectivity of **1a** was evaluated by fluorescence titration with 10 different ions (Figure 2b). Interestingly a negligible change in the  $R$  value was induced by the metal ions, except for  $\text{Ag}^+$ . Furthermore, **1a** showed a large increase in  $R$  value upon the addition of  $\text{Ag}^+$  ( $50 \mu\text{M}$ ) in the presence of a 10-fold excess of the other metal ions ( $500 \mu\text{M}$ ), which is indicative of the significantly low binding affinity of **1a** toward the other metal ions ( $K_a < 10^4 \text{ M}^{-1}$ ). These data clearly indicate that **1a** is a selective ratiometric chemosensor for  $\text{Ag}^+$ . Because it was reported that 4,10-diaza-15-crown 5-ether has a strong binding affinity toward various metal ions ( $\log K$  for  $\text{Ag}^+$ ,  $\text{Cu}^{\text{II}}$ ,  $\text{Cd}^{\text{II}}$ , and  $\text{Zn}^{\text{II}}$  is 5.85, 7.17, 8.72, and 5.34, respectively),<sup>5</sup> the high sensing selectivity of **1a** toward  $\text{Ag}^+$  might be attributable to the restricted rigid conformation of the cyclic aza crown ether, which exclusively binds to  $\text{Ag}^+$ .

The sensing mechanism of **1a** toward  $\text{Ag}^+$  was next examined. For structural analysis, the readily available **2a** was prepared as an anthracene analogue of **1a**. We confirmed that **2a** also gave a large-emission red shift (from 417 to 452 nm,  $\Delta\lambda_{\text{em}} = 35 \text{ nm}$ ,  $1857 \text{ cm}^{-1}$ ) upon binding to  $\text{Ag}^+$  (Figure S4 in the SI). Figure 3a shows the structure of the **2a**- $\text{Ag}^+$  complex, which was determined by X-ray crystallographic analysis. In this complex,  $\text{Ag}^+$  is located adjacent to the upper  $\pi$  plane of the anthracene ring by coordination with all of the N and O atoms of the diaza-15-crown ether. The distance between  $\text{Ag}^+$  and the nearest neighbor C9 atom is 2.46 Å, which is much smaller than the sum of the van

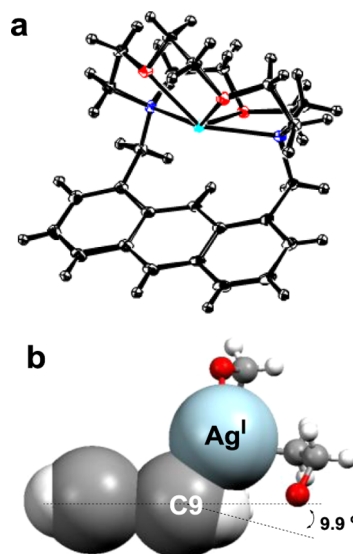


**Figure 3.** X-ray crystallographic analysis of **2a**- $\text{Ag}^+$  ( $\text{C}_{26}\text{H}_{32}\text{N}_2\text{O}_7\text{ClAg}$ ). (a) Perspective view with 50% probability ellipsoids. (b) Cross-sectional view of **2a**- $\text{Ag}^+$ . The perchlorate anion is omitted for clarity.

der Waals radii of  $\text{Ag}^+$  (1.72 Å) and an aromatic C (1.77 Å). This short distance may imply the formation of a metal- $\pi$  interaction as proposed for previously reported  $\text{Ag}^+$  complexes.<sup>6</sup> Figure 3b shows a cross-sectional view of the **2a**- $\text{Ag}^+$  complex. It is apparent that  $\text{Ag}^+$  is in very close contact with C9. Interestingly, this close contact induces bending of the C9-H bond by  $9.9^\circ$  from the planar  $\pi$  plane of the anthracene ring toward the opposite side to  $\text{Ag}^+$ .

In the  $^{13}\text{C}$  NMR spectrum (Figure S5 in the SI), C9 of **2a** significantly shifted upfield from 123.3 to 107.3 ppm ( $\Delta\delta = 16 \text{ ppm}$ ) upon coordination with  $\text{Ag}^+$ , while the other aromatic C atoms shifted downfield slightly ( $\Delta\delta = 0.8\text{--}3.7 \text{ ppm}$ ). In the  $^1\text{H}$  NMR spectrum (Figure S6 in the SI), H9 shifted slightly ( $\Delta\delta = 0.01 \text{ ppm}$ ) upon complexation with  $\text{Ag}^+$ , while the other aromatic H atoms shifted significantly downfield ( $\Delta\delta = 0.15\text{--}0.30 \text{ ppm}$ ). The unique chemical shift changes of C9 and H9, which are distinct from those of the other atoms, suggest that  $\text{Ag}^+$  is located in a position proximate to C9 of the anthracene ring in the solution state.

In the optimized structure calculation by the density functional theory (DFT) method (Figure S7 and Tables S7 and S8 in the SI), the binding energy of  $\text{Ag}^+$  with ligand **2a** was evaluated to be 106.8 kcal/mol (Table S4 in the SI), the value of which is almost the same as that of 4,10-diaza-15-crown 5-ether lacking the anthracene moiety (107.1 kcal/mol). In addition, the number of 4d electrons of **2a**- $\text{Ag}^+$  was predicted to be 9.94 by natural bond orbital analysis (Table S5 in the SI), the value of which is almost the same as that of the  $\text{Ag}^+$  complex of 4,10-diaza-15-crown 5-ether (9.95). These results suggest that the anthracene ring does not contribute to stabilizing the  $\text{Ag}^+$  complex through bonding interaction. In time-dependent DFT calculation, the electric-dipole-allowed  $S_0 \rightarrow S_1$  transition energy of **2a** was calculated as 3.57 eV, while the same transition energy for the **2a**- $\text{Ag}^+$  complex was calculated as 3.41 eV, which is 0.16 eV lower than that of **2a** (Figure S8 and Tables S6, S9, and S10 in the SI). This result reasonably reproduces the experimentally observed  $\text{Ag}^+$  ion-induced red shift of the absorption band [**2a** 3.39 eV (366 nm)  $\rightarrow$  **2a**- $\text{Ag}^+$  3.24 eV (383 nm)]. Interestingly, when the calculation was performed for **2a** at the optimized geometry of the **2a**- $\text{Ag}^+$

complex (Table S6 in the SI), the  $S_0 \rightarrow S_1$  transition energy was calculated as 3.50 eV, which is 0.07 eV lower than that of **2a** at its original optimized geometry ( $\Delta E = 3.57$  eV).<sup>7</sup> Therefore, the red shift of **2a** can be mainly ascribed to the electronic perturbation and/or the structural deformation of anthracene, as shown in Figure 3b, upon coordination with the  $\text{Ag}^{\text{I}}$  cation. Further theoretical analysis is in process and will be reported elsewhere.

The  $\text{Ag}^{\text{I}}$  complex of the ratiometric probe **1a** was used for detection of the cyanide ion ( $\text{CN}^-$ ) in an aqueous medium.  $\text{CN}^-$  is a well-known toxic anion that is poisonous to biological systems. Therefore, effective detection methods for  $\text{CN}^-$  have been developed,<sup>8</sup> especially for the environmental analysis of plant effluent. It was found that the **1a-Ag<sup>I</sup>** complex exhibited a clear emission blue shift by KCN under aqueous buffer conditions (50 mM phosphate buffer, pH 8.0; Figure 4). This

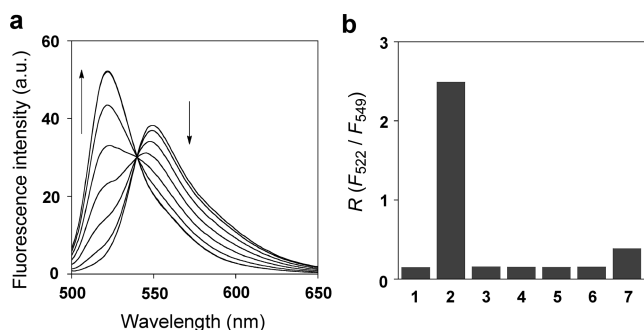


**Figure 4.** (a) Fluorescence spectral change of **1a-AgI** ( $6 \mu\text{M}$ ) upon the addition of cyanide anion (0–2 equiv). 50 mM phosphate buffer (pH 8.0),  $\lambda_{\text{ex}} = 488$  nm,  $25^\circ\text{C}$ . (b) Fluorescence sensing selectivity of **1a-AgI** ( $6 \mu\text{M}$ ) among various anion (1: none, 2: KCN  $14 \mu\text{M}$ , 3: KCl  $200 \mu\text{M}$ , 4:  $\text{CH}_3\text{COONa}$   $200 \mu\text{M}$ , 5:  $\text{Na}_2\text{CO}_3$   $200 \mu\text{M}$ , 6:  $\text{Na}_2\text{SO}_4$   $200 \mu\text{M}$ , 7:  $\text{NaSCN}$   $200 \mu\text{M}$ ). Conditions; 50 mM phosphate buffer (pH 8.0),  $\lambda_{\text{ex}} = 488$  nm,  $25^\circ\text{C}$ .

wavelength shift caused a large increase in the ratio  $R (F_{522}/F_{549})$  from 0.15 to 2.46. Electrospray ionization time-of-flight mass spectrometry analysis indicated that the cyanide ion enhanced decomplexation of  $\text{Ag}^{\text{I}}$  from **1a-Ag<sup>I</sup>** to release the  $\text{Ag}^{\text{I}}$ -free ligand **1a** because of the formation of a stable  $\text{AgCN}$  salt (Figure S9 in the SI). The detection limit for  $\text{CN}^-$  was calculated as  $0.47 \mu\text{M}$  ( $3\sigma$ ) under the same conditions. As shown in Figure 4b, **1a-Ag<sup>I</sup>** gave good sensing selectivity toward  $\text{CN}^-$  among various anion species such as chloride, acetate, carbonate, sulfate, and thiocyanate. These data revealed that **1a-Ag<sup>I</sup>** is a useful ratiometric chemosensor for the cyanide ion with a clear and selective fluorescence response, which has not been readily achieved by current  $\text{CN}^-$  probes.<sup>8</sup>

In conclusion, we have developed a ratiometric fluorescent probe for  $\text{Ag}^{\text{I}}$  based on a new design strategy, which consists of a conformationally restricted aza crown ether as a binding unit and an arene–metal ion interaction as a sensing mechanism. The probe had high sensing selectivity toward  $\text{Ag}^{\text{I}}$  with a large-emission red shift, which is expected to be useful in environmental analyses as well as in the elucidation of biological functions of  $\text{Ag}^{\text{I}}$ .<sup>9</sup> Apart from metal-ion sensing, the  $\text{Ag}^{\text{I}}$  complex **1a-Ag<sup>I</sup>** was also used in the ratiometric detection of cyanide anions, further demonstrating the versatility of the present probe design in fluorescence analysis. We envision that structural modification of the cyclic ligand unit can provide new ratiometric probes with high sensing selectivity toward other metal ions. Our research into this aspect is ongoing.

## ■ ASSOCIATED CONTENT

### Supporting Information

Synthetic procedures and photophysical properties of compounds, experimental details of computational calculation, absorption spectral changes of **1a** and **1b** upon the addition of  $\text{Ag}^{\text{I}}$ , Job's plots, fluorescence spectral change of **2a-Ag<sup>I</sup>**,  $^1\text{H}$  and  $^{13}\text{C}$  NMR and mass spectra, and X-ray crystallographic data for complex **2a-Ag<sup>I</sup>** in CIF format. This material is available free of charge via the Internet at <http://pubs.acs.org>.

## ■ AUTHOR INFORMATION

### Corresponding Author

\*E-mail: [ojida@phar.kyushu-u.ac.jp](mailto:ojida@phar.kyushu-u.ac.jp).

### Notes

The authors declare no competing financial interest.

## ■ ACKNOWLEDGMENTS

This work was performed under the Cooperative Research Program of “Network Joint Research Center for Materials and Devices”. A.O. acknowledges the Toray Science Foundation for its financial support. I.T. acknowledges the Japan Society for the Promotion of Science Research Fellowships for Young Scientists.

## ■ REFERENCES

- (1) (a) de Silva, A. P.; Nimal Gunaratne, H. Q.; Gunnlaugsson, T.; Huxley, A. J. M.; McCoy, C. P.; Rademacher, J. T.; Rice, T. E. *Chem. Rev.* **1997**, *97*, 1515–1566. (b) Domaille, D. W.; Que, E. L.; Chang, C. J. *Nat. Chem. Biol.* **2008**, *4*, 168–175. (c) Prodi, L.; Montalti, M.; Zaccheroni, N.; Dolci, L. S. *Topics in fluorescence spectroscopy*; Springer: New York, 2005; Vol. 9, pp 1–52. (d) Zhang, J. F.; Zhou, Y.; Yoon, J.; Kim, J. S. *Chem. Soc. Rev.* **2011**, *40*, 3416–3429.
- (2) Takashima, I.; Kinoshita, M.; Kawagoe, R.; Nakagawa, S.; Sugimoto, M.; Hamachi, I.; Ojida, A. *Chem.—Eur. J.* **2014**, *20*, 2184–2192.
- (3) Jang, H. O.; Nakamura, K.; Yi, S.-S.; Kim, J. S.; Go, J. R.; Yoon, J. J. *Inclusion Phenom. Macrocyclic Chem.* **2001**, *40*, 313–316.
- (4) Recent examples of the ratiometric fluorescent probes for  $\text{Ag}^{\text{I}}$ : (a) Wang, H.-H.; Xue, L.; Qian, Y.-Y.; Jiang, H. *Org. Lett.* **2010**, *12*, 292–295. (b) Wang, F.; Nandhakumar, R.; Moon, J. H.; Kim, K. M.; Lee, J. Y.; Yoon, J. *Inorg. Chem.* **2011**, *50*, 2240–2245.
- (5) Izat, R. M.; Bradshaw, J. S.; Nielsen, S. A.; Lamb, J. D.; Christensen, J. J. *Chem. Rev.* **1985**, *85*, 271–339.
- (6) Munakata, M.; Wu, L. P.; Ning, G. L. *Coord. Chem. Rev.* **2000**, *198*, 171–203.
- (7) The  $S_0 \rightarrow S_1$  transition energy of ligand **2a** with the optimized geometry of the **2a-Ag<sup>I</sup>** complex ( $\Delta E = 3.50$  eV) did not change upon coordination of a positive charge (+1.0 e) to its aza crown unit ( $\Delta E = 3.51$  eV; Table S6 in the SI), implying that electrostatic interaction between anthracene and the  $\text{Ag}^{\text{I}}$  cation does not largely contribute to the red shift.
- (8) (a) Badugu, R.; Lakowicz, J. R.; Geddes, C. D. *J. Am. Chem. Soc.* **2005**, *127*, 3635–3641. (b) Chung, S.-Y.; Nam, S.-W.; Lim, J.; Park, S.; Yoon, J. *Chem. Commun.* **2009**, 2866–2868. (c) Xu, Z.; Pan, J.; Spring, D. R.; Cui, J.; Yoon, J. *Tetrahedron* **2010**, *66*, 1678–1683.
- (9) (a) Liao, S. Y.; Read, D. C.; Pugh, W. J.; Furr, J. R.; Russell, A. D. *Lett. Appl. Microbiol.* **1997**, *25*, 279–283. (b) Kascatan-Nebioglu, A.; Melaiye, A.; Hindi, K.; Durmus, S.; Panzner, M. J.; Hogue, L. A.; Mallett, R. J.; Hovis, C. E.; Coughenour, M.; Crosby, S. D.; Milsted, A.; Ely, D. L.; Tessier, C. A.; Cannon, C. L.; Youngs, W. J. *J. Med. Chem.* **2006**, *49*, 6811–6818. (c) Ono, A.; Cao, S.; Togashi, H.; Tashiro, M.; Fujimoto, T.; Machinami, T.; Oda, S.; Miyake, Y.; Okamoto, I.; Tanaka, Y. *Chem. Commun.* **2008**, 4825–2827.